Using Synthetic Cyclone Models For High Wind GNSS-R Calibration, Validation And Algorithm Development: A CYGNSS Case Study

Mohammad M. Al-Khaldi, *Member, IEEE,* Scott Gleason, *Senior Member, IEEE,* Joel T. Johnson, *Fellow, IEEE,* Rajeswari Balasubramaniam, *Member, IEEE,* Christopher Ruf, *Fellow, IEEE,* Darren S. McKague, *Member, IEEE,* Bachir Annane, Tianlin Wang, *Member, IEEE,* Anthony Russel and Dorina Twigg

***Abstract*—This work reports a case study of the use of synthetic cyclone models for the development, assessment and validation of GNSS-R wind speed remote sensing algorithms using a CYGNSS data record extending from August 1st, 2018 to December 31st, 2022. Synthetic cyclone models are shown to be useful in assessing the high wind speed sensitivity of CYGNSS's v1.0, v2.1, v3.0, v3.1, and future v3.2 normalized bistatic radar cross section (NBRCS) products due to the extended matchup dataset of high wind speed information that is obtained. The models are also shown useful in investigating the impacts of specific error corrections terms and in the development of Level-2 geophysical model functions for the retrieval of ocean surface winds.**

***Index Terms*—Cyclone global navigation satellite system, CYGNSS, Global Navigation Satellite Systems Reflectometry (GNSS-R), synthetic storm models, Level-1 calibration, Level-2 ocean wind speed retrieval algorithm development, microwave remote sensing**

I. Introduction

THE retrieval of ocean surface wind speed [1]–[6] is a core mission objective in many global navigation satellite system-reflectometry (GNSS-R) missions such as NASA's Cyclone Global Navigation Satellite System (CYGNSS) mission [7]. The CYGNSS mission launched an eight satellite constellation of receivers into low earth orbit in 2016. Each satellite is equipped with a Delay Mapping Receiver (DMR) primary science payload [8] that observes the reflections of Global Positioning System (GPS) transmissions from Earth's surface. Because contact was lost with CYGNSS flight module (FM) 6 in November 2022, the constellation now consists of seven receivers. Each receiver is capable of tracking up to 4 GPS reflections off the Earth's surface so that the constellation produces a total of 28 (originally 32) simultaneous measurements over the 1000 msec (prior to August 2019) or 500 msec (after August 2019) integration period of a single measurement. The 1.575 GHz frequency of the GPS L1 Coarse/Acquisition (C/A) signals used makes CYGNSS measurements insensitive to cloud cover and rain attenuation, even in heavy rain rates [9], allowing CYGNSS to provide the all-weather operation and frequent revisit [10] needed to provide deeper insights into cyclone development and evolution [11].

CYGNSS's measurements are impacted by multiple sources of uncertainty [12]–[16] that are corrected when producing the mission's calibrated Level-1 products from which downstream Level-2 ocean wind speeds are derived. Because the CYGNSS mission team continues to develop improved calibration processes, matchup datasets that provide information on "true" ocean wind speeds remain valuable to the mission team [17]. The availability of matchup datasets is a particular issue for wind speeds that exceed 20 m/s due to the relative infrequency of these wind speeds and limitations in existing matchup datasets for high wind speeds.

This work explores the utility of synthetic cyclone models in CYGNSS Level-1 calibration algorithm and Level-2 retrieval algorithm development. The next Section overviews CYGNSS's Level-1 calibration algorithm, and Section III discusses the means with which Level-1 observables may be used for the retrieval of ocean surface winds and the limitations associated with existing reference datasets at high winds. Section IV describes the synthetic storm model used in the analysis, and Section V describes uses of the model in the context of CYGNSS calibration, validation and algorithm development activities. Section VI then provides concluding remarks.

II. Level-1 Calibration of CYGNSS's Observables

CYGNSS's standard delay-Doppler Map (DDM) measurements are first produced in uncalibrated L0 "raw count" units by downlinking a 17 (delay) $\times$ 11 (Doppler) set of points $C(\tau, f)$ cropped from the 128 $\times$ 20 DDM formed onboard each receiver. A first set of "L1a" calibration steps are applied to $C(\tau, f)$ to convert it into an absolute power DDM in watts

$$P_g(\tau, f) = \frac{\left(C(\tau, f) - NC_{NDR} \cdot C_N\right)\left(P_B + P_r\right)}{C_B} \quad (1)$$

Here C_N represents internal and external noise power contributions that are subtracted from the received counts to obtain the reflected power. C_N is computed as the mean value of the counts in the first 45 "early time" delay rows of the

The research of this article is funded by the NASA Science Mission Directorate through the University of Michigan under Contract NNL13AQ00C.

M. M. Al-Khaldi, J. T. Johnson and T. Wang are with the Department of Electrical and Computer Engineering and ElectroScience Laboratory, The Ohio State University, Columbus, OH 43210 USA.

S. Gleason is with DAAXA LLC, Boulder, CO 80307 USA.

R. Balasubramaniam, C. Ruf and D. S. McKague are with the Department of Climate and Space Sciences and Engineering, University of Michigan, Ann Arbor, MI 48109 USA.

B. Annane is with Univ. of Miami/CIMAS and NOAA/AOML/HRD, Miami, FL 33149 USA

A. Russel and D. Twigg are with the Space Physics Research Laboratory, University of Michigan, Ann Arbor, MI 48109 USA.

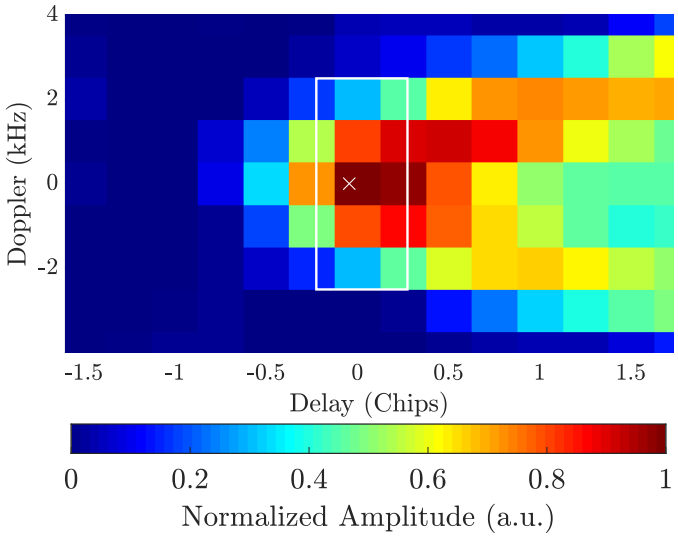

Fig. 1: Normalized Level-1 DDM measured by CYG01 tracking PRN 11 over 30.5°N 172.38°E on DOY 256, 2018. Reference ECMWF surface winds estimated to be ≈8.9 m/s.

full onboard DDM in which no ocean reflected signals should be present. The term NC_{NDR} represents a multiplicative correction to this noise level estimate [14] defined as

$$NC_{NDR} = 1 - S_{NDR}\left(1 - \Gamma_{ref}\left(BR_{noise}\right)\right) \tag{2}$$

that accounts for discretization effects in CYGNSS's 2 bit Analog-to-Digital Converter (ADC) in the presence of signal power level biases. These effects are described by the function Γ_{ref} that depends on 'bin ratios' (BR_{noise}) observed in the ADC. BR_{noise} describes the ratio of the number of samples within states ±1 to the number of samples within states ±3 over a 1 second period. As specified in [14], Γ_{ref} can be determined as a function of BR_{noise} to eliminate ADC-induced calibration biases using end-to-end simulations of the on-board instrument. The final scale factor S_{NDR} is defined so that a value of 0 translates to no correction being applied and a value of 1 results in the full Γ_{ref} correction.

Equation (1) also involves the thermal noise power levels P_B and P_r in Watts for the reference blackbody load and the receiver, respectively. The former is known through onboard measurements of the blackbody load physical temperature while the latter is obtained using pre-launch parameterizations as a function of physical temperature. Finally, C_B represents the counts measured when the receiver is switched to observe the blackbody load. Equation (1) shows that CYGNSS's "L1a" calibration is fundamentally concerned with correcting for noise levels and instrument gain as a function of varying internal temperature.

The second "L1" stage of CYGNSS's calibration algorithm corrects for a wide range of other observation geometry and GPS transmit power level terms to obtain a Normalized Bistatic Radar Cross Section (NBRCS). By assuming that the forward propagation paths and the projection of CYGNSS's receive antenna patterns onto the surface do not vary appreciably within the L1 DDM's maximum extent, a BRCS $\sigma(\tau, f)$ DDM in square meters is first computed by inverting the bistatic radar equation:

$$\sigma(\tau, f) = \frac{(4\pi)^3}{\lambda^2}\frac{1}{EIRP}\frac{P_g(\tau, f)R_T^2 R_R^2 L_a}{G_R} \tag{3}$$

in which the range from the specular point to the transmitter R_T and receiver R_R, the CYGNSS antenna gain at the specular point G_R, any atmospheric loss L_a, the electromagnetic wavelength λ, and the varying Effective Isotropic Radiated Power (EIRP) of the GPS satellite toward the specular point are all assumed known. The EIRP can also be estimated using signal power measurements P_Z from the zenith antenna and an inversion of the Friis transmission formula:

$$\text{EIRP} = P_T \cdot G_T \tag{4}$$

$$= \frac{\left(4\pi R_{LOS}\right)^2}{\lambda^2} \cdot \frac{NC_z \cdot P_z}{G_{LNA}^z \cdot G_R^Z \cdot \text{ZSR}} \tag{5}$$

in which R_{LOS} is the direct path range from the transmitter to the receiver, G_R^Z is the CYGNSS zenith antenna gain toward the GPS satellite at incidence and azimuth angles θ_Z and ϕ_Z, and ZSR represents the ratio of the GPS EIRP toward CYGNSS as compared to that towards the specular point. Finally G_{LNA}^Z accounts for the temperature dependence of the zenith antenna low noise amplifier, while NC_z is a bin-ratio correction analogous to that in Equation (2).

A smaller subset of pixels within $\sigma(\tau, f)$ are then averaged to form a Delay Doppler Map Average (DDMA) that is later normalized by an equivalent effective scattering area DDM $\overline{A}$ to obtain an NBRCS:

$$\sigma_0 = \frac{\sum_{i=-1}^{1}\sum_{j=-2}^{2}\sigma(\tau_T + i, f_T + j)}{\sum_{i=-1}^{1}\sum_{j=-2}^{2}\overline{A}(\tau_T + i, f_T + j)} \tag{6}$$

where τ_T and f_T are the specular bin (or tracking point) delay and Doppler indices, respectively. For CYGNSS, the DDMA is computed over a 3×5 pixel region with resolutions $\Delta\tau$ = 0.25 chips (1 chip ≈ 0.97μs) and Δf = 500 Hz per pixel, centered on the tracking point as indicated by the white box in Fig. 1.

Estimates of the scattering area $\overline{A}(\tau, \text{f})$ are obtained using forward models describing the total physical area satisfying the delay/Doppler limits for a given DDM pixel (as specified by the Woodward Ambiguity function)

$$\overline{A}(\tau, f) = \iint \Lambda^2(\tau - \tau')S^2(f - f')dxdy \tag{7}$$

The process is typically repeated for a wide range of receiver elevations, incidence angles, and azimuth rotation angles to form a reference scattering area look up table (LUT) such that reported areas are predictions of anticipated footprints as opposed to being direct retrievals of scattering range cells.

The CYGNSS mission has released multiple Level 1 data products as calibration processes have continued to improve. The differences between these data products can be described as related to:

• the version of the nadir antenna pattern G_R used. Prelaunch gain pattern measurements (performed prior to the mounting of the science antenna arrays in the flight modules) have been refined in subsequent releases through tuning based either on

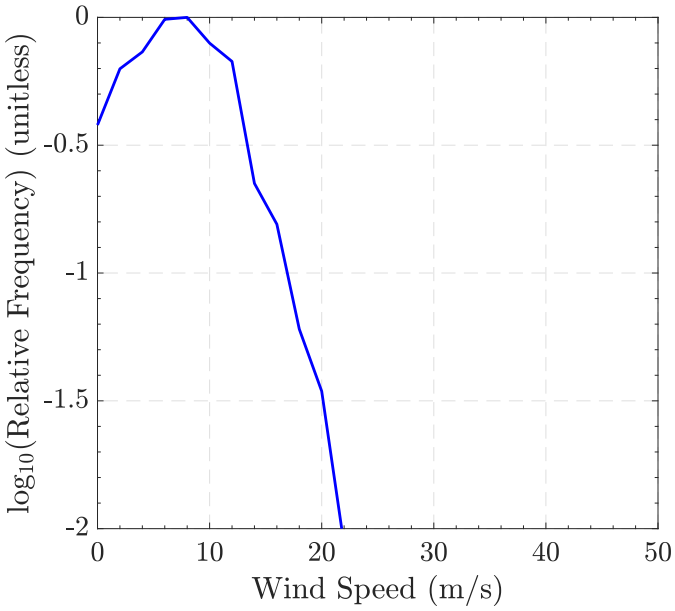

Fig. 2: Probability density function (PDF) communicating ERA-5 wind reports for specular observations estimated to have occurred within a 50 km radius of cyclone center at the time of observation. The PDF combines data for all cyclones occurring within CYGNSS's coverage over a 1 year data record

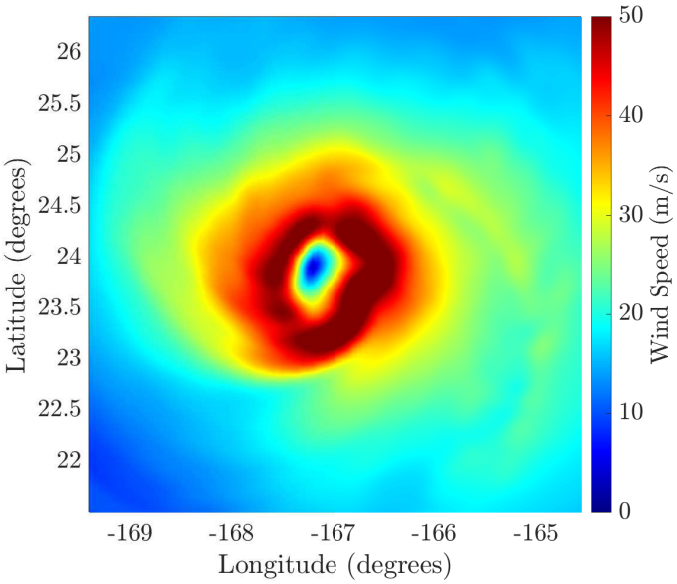

Fig. 3: Example HWRF wind field in current use for Level-2 CYGNSS algorithm development. The wind field describes the structure of Hurricane Walaka on DOY 277, 2018 at 06:00:00 UTC

Level 2 wind speed matchups or on model-based predictions of NBRCS values based on ocean wind speed and/or wave matchup datasets. An additional approach used in v3.2 emphasizes achieving a uniform NBRCS, given comparable surface conditions, across all receive channels.

• the EIRP estimates used. Early CYGNSS releases assumed a static EIRP level. However, the analyses described in [15], [16] highlighted the need to track EIRP levels in real-time given the relative frequency of commanded GPS EIRP variations. The repurposing of the CYGNSS zenith antennas into direct power monitors in August 2018 allowed the dynamic EIRP correction described in equation (5) to be used in subsequent releases.

• the inclusion of the bin-ratio correction for the nadir antenna. Reference [14] shows that NBRCS offsets in excess of 50% given comparable surface conditions can occur due to these effects. The initial correction used in CYGNSS's v3.1 data was removed in v3.2 (see Section V-B) and a refined version is under development for v3.3.

• the inclusion of the bin-ratio correction for the zenith antenna. Thse effects have also been shown to compromise real-time EIRP estimates and attempts to compensate for related degradation as a function of zenith bin ratios have been attempted.

• the correction of thermal variations in the zenith antenna. Recent investigations [18] have noted non-geophysical temporal oscillations dominated by a 42-60 day sinusoidal component in CYGNSS's observables. Root cause analyses have identified thermal variations in the zenith antenna as contributing, so that a revised zenith LNA gain vs temperature table is included in v3.2.

III. Level-2 Ocean Wind Speed Retrieval Algorithm Development

The retrieval of ocean surface winds using CYGNSS's observables, namely NBRCS and/or Leading Edge Slope (LES) estimates, requires the inversion of either physically-based [19], [20] or empirically-based [21] models that relate these quantities to surface wind speeds. The Geometrical Optics approximation of incoherent forward scattering from a rough surface is the most commonly applied physically-based model, and relates the NBRCS to the surface mean square slope [22], [23]. While the GO is successful at describing the overall trends of received power as a function of surface winds, it achieves reduced efficacy in predicting received power levels when compared to an empirical data driven approach. The empirical approach used in CYGNSS's Level-2 ocean wind speeds [21] uses co-locations of CYGNSS's NBRCS measurements with reference wind speed estimates to derive an empirical Geophysical Model Function (GMF) relating the two quantities given parameters such as the incidence angle, specific receive channel, CYGNSS receiver/transmitter pair, and/or ancillary wave information such as the significant wave height. Given the emphasis in this work on Level 1 calibration processes and to simplify the discussion, the CYGNSS NBRCS in examined in what follows as a function of wind speed alone.

The need for coincident wind speeds in deriving the GMF places particular emphasis on the quality of the reference wind speed datasets used. The CYGNSS mission currently uses winds from the the latest generation of the European Centre for Medium-Range Weather Forecasts (ECMWF) reanalysis product, ERA5 [24]. The product incorporates historical and contemporary observations from spaceborne receivers, airborne campaigns, and in situ sensors into global assimilation systems to produce surface wind components (10 meter u-

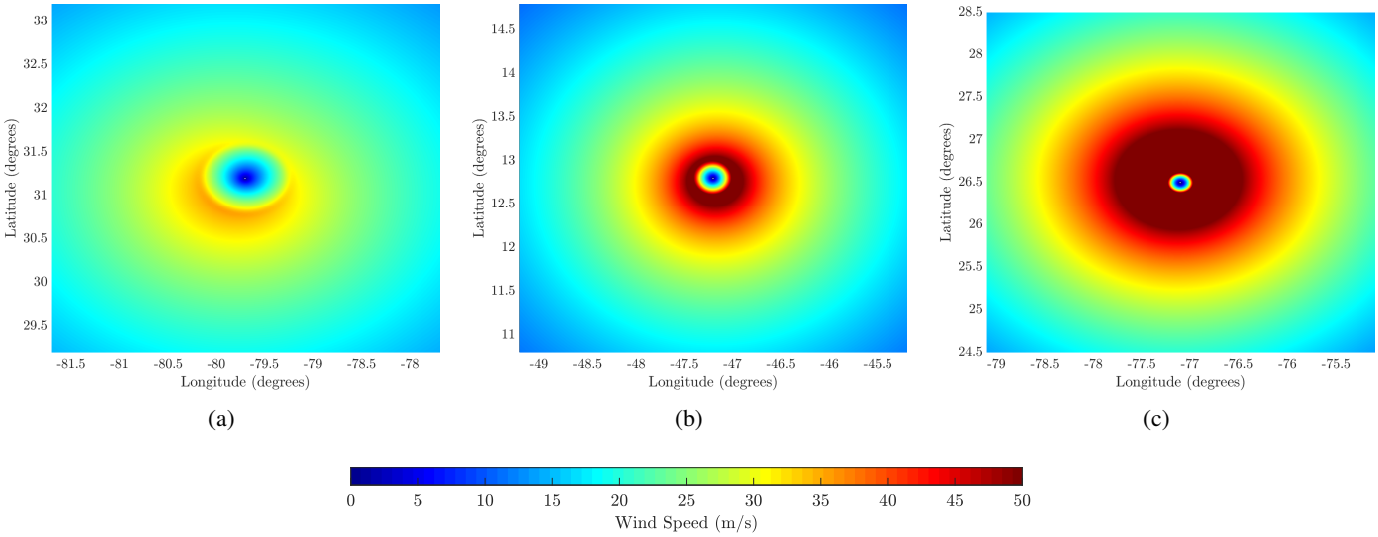

Fig. 4: Example Willoughby model wind fields (a) Cat 1, Hurricane Isaias on DOY 216, 2020 (b) Cat 3, Hurricane Sam on DOY 268, 2021 (c) Cat 5, Hurricane Dorian on DOY 244, 2019

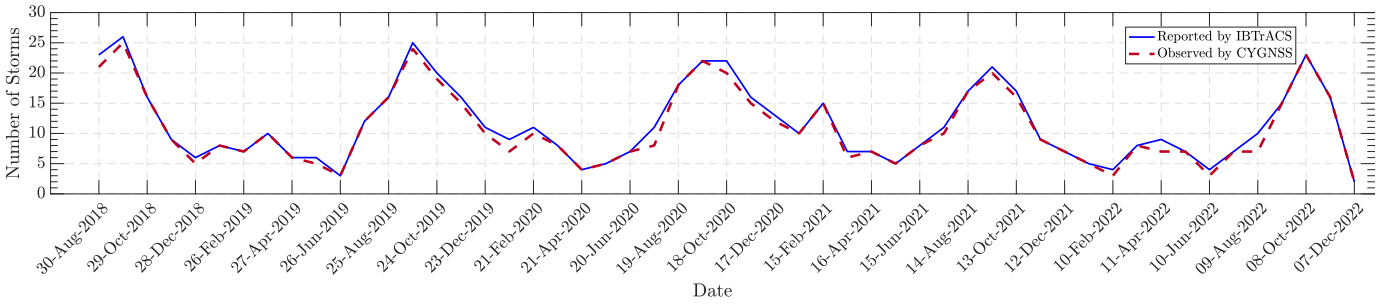

Fig. 5: Time series capturing the total number of unique storms reported by IBTrACS and observed by CYGNSS

component and 10 meter v-component) projected on hourly, uniformly sampled 0.25×0.25 degree (≈25 km resolution) latitude/longitude maps. The available data record extends from 1979 to the present with a latency that is on the order of 5 days and 3 months for preliminary and final releases respectively. The hourly record the dataset provides with root-mean-square-errors (RMSEs) on the order of 1.2-2.3 m/s [25], [26] relative to *in situ* observations has motivated its use in the development of CYGNSS's Level-2 retrieval algorithms for wind speed retrievals up to 20-30 m/s. Retrievals in this wind speed regime are labeled "Fully Developed Seas" (FDS) winds.

A probability density function of ERA5 wind speeds within a 50 km radius of all Category 1 or greater cyclones observed by CYGNSS over a 1 year period is shown in Figure 2. The small probabilities of wind speeds greater than 30 m/s in Figure 2 indicates limitations in the ERA5 matchup data at higher wind speeds. These limitations are attributable in part to the strict data quality control enforced in the ERA product that reduces confidence in higher wind speed input data [27]. These issues motivate the identification of alternate matchup datasets for GMF development under high wind conditions.

The CYGNSS mission also retrieves wind speeds using a second Young Seas Limited Fetch (YSLF) GMF that is intended to better represent the NBRCS under high wind speed conditions. Reference wind speeds for the development of the YSLF GMF have previously been obtained from the stepped frequency microwave radiometer (SFMR) on board NOAA's hurricane hunter aircraft [28]. The use of aircraft reference data however is challenged by the limited amount of data available and by the differences in spatial resolution between spaceborne and airborne observations. Other potential sources of high wind reference wind fields include commercial cyclone data such as that provided by Oceanweather, Inc (OWI) [29] or by the Hurricane Weather Research and Forecasting (HWRF) model; sample HWRF wind speeds for Hurricane Wakala on Day Of Year (DOY) 277 during 2018 are shown in Figure 3. While these wind fields shown improved properties, their greater costs, increased latency, temporal resolution of 3 hours or coarser, and limited availability to end users remain challenging.

It is important to reiterate that in what follows, the proposed use of synthetic cyclone models for GNSS-R calibration, validation and algorithm development is exclusively concerned with high wind speed observation scenarios. The use of ERA5 as a reference set for observation scenarios where the 'FDS' L2 algorithm is applicable continues to be a preferred approach. The proposed work is intended to address the need for reference data not met by model winds for observation scenarios where the 'YSLF' L2 algorithm applies (see Fig.

TABLE I: Description of major L1 calibration differences across different CYGNSS data releases. u_{10} refers to a wind based tuning, σ_0^M refers to a model NBRCS based tuning, $\overline{\sigma_0}$ refers to a tuning approach that minimizes NBRCS variability across the different receive channels. For EIRP definition see (5), for NC_{NDR} definition see (2). G_{LNA}^{Z} are the set of channel specific zenith LNA gains and G_R are the set of channel specific nadir antenna gain patterns.

Data Version	EIRP	NC_{NDR}	NC_Z	G_{LNA}^{Z} Version	G_R Version	G_R Tuning
v1.0	Static	×	×	Prelaunch	1	N/A
v2.1	Static	×	×	Prelaunch	6	u_{10}
v3.0	Measured	×	×	Prelaunch	9	σ_0^M
v3.1	Measured	✓	✓	Prelaunch	17	σ_0^M
v3.2	Measured	×	✓	Revised	20	$\overline{\sigma_0}$

2).

IV. Overview of Synthetic Cyclone Models

Given the challenges identified in the preceding section, the use of synthetic cyclone models appears to be a desirable alternate method for producing high wind speed matchup datasets. Synthetic cyclone models provide a representation of wind speeds within a specified radius of a cyclone's center, and have been used in many applications including storm surge predictions and in the design of coastal protection measures [30]–[32]. Other recent works have examined their use in improving the retrieval of high wind speed wind fields from CYGNSS measurements [11]. A variety of synthetic cyclone models have been reported in the literature; in what follows, the Willoughby storm model [33], [34] is adopted given its reasonable accuracy in reproducing wind speeds within several hundred kilometers of a cyclone's center while retaining a simple analytical form.

The model is expressed solely in terms of the latitude φ and longitude θ of the cyclone center at time t, the maximum Sustained Surface Wind (SSW) V_{max} of the cyclone, the speed of the cyclone center's translational motion V_t and the compass angle θ_t of this motion. References [33], [34] then provide equations that determine the quantities R_{max}, n, X_1, X_2, A and ω from V_{max} and φ. For a translating storm, the output wind speed V_f is determined as [35]:

$$V_f = \sqrt{(-V_m \cos\theta_t)^2 + \left[\frac{V_t \sin\theta_t}{R_{max}^2 + r^2}\right]^2} \tag{8}$$

in which V_m is specified as V_{in}, V_{out}, or V_{tr} depending on the distance of a point from the cyclone center. V_{in} is used for wind speeds within radius R_{max} of the cyclone center

$$V_{in}(r) = V_{max}\left(\frac{r}{R_{max}}\right)^n \tag{9}$$

where r is the radial separation from the storm's center to a surface point. V_{out} then describes surface winds for distances greater than $R_{max} + 25$ km as

$$V_{out}(r) = V_{max}\left[(1-A)e^{-\frac{r-Rmax}{X_1}} + Ae^{-\frac{r-Rmax}{X_2}}\right] \tag{10}$$

Wind speeds within R_{max} and $R_{max} + 25$ km are finally a mixture of the winds in the inner and outer domains weighted by ω.

$$V_{tr}(r) = V_{in}(1-\omega) + \omega V_{out} \tag{11}$$

Example Willoughby renditions of hurricanes observed by the CYGNSS constellation are depicted in Fig. 4.

The storm center location and V_{max} time history information required by the Willoughby model is obtained from the International Best Track Archive for Climate Stewardship (IBTrACS) dataset [36]. This dataset unifies global storm best track data derived from a variety of sources such as HURDAT, ATCF, JAMA and others into a single self contained data release. Figure 5 plots the number of cyclones per month obtained using the IBTrACS dataset from August 1st 2018 to December 31st 2022 and the corresponding number having CYGNSS coverage within the same period. A cyclone is deemed to have been observed by CYGNSS when any specular point lies within +/- 250 km of cyclone center within +/- 15 minutes of the overpass. The extensive high wind matchup dataset provided by the synthetic storm approach is evident in Figure 5.

V. Applications of Synthetic Storm Models For GNSS-R L1 Calibration Assessment, Tuning and Level-2 Algorithm Development

A. Use For Level-1 Calibration Assessment

In this Section, IBTrACS/Willoughby wind fields are applied in studies of CYGNSS's Level-1 and Level-2 processing. Level-1 studies examine calibration approaches used in the v1.0, v2.1, v3.0, v3.1 and v3.2 releases. Differences in these releases involve the EIRP, zenith bin ratio, receive antenna gain pattern, nadir bin ratio, and thermal corrections as discussed previously and as summarized more specifically in Table I.

Wind speed matchup datasets for CYGNSS measurements were generated by interpolating IBTrACS cyclone center and maximum wind data in time from the original 3, 6, or 12 hour interval into a 1 second time sampling used to generate Willoughby model wind fields. Storm locations and maximum winds are linearly interpolated between reporting intervals to provide this 1 second information. It is acknowledged that some storms can undergo rapid intensification over various phases of their life cycle such that this simple interpolation may not always be representative of their true behaviour at the time of observation. CYGNSS specular points within 250 km of cyclone center within a +/-15 minute window were then identified, and the corresponding IBTrACS/Willoughby model wind speeds compiled at the specular point location. The final dataset obtained from this process can then be binned versus the matchup wind speed, and the mean μ_{NBRCS} and standard

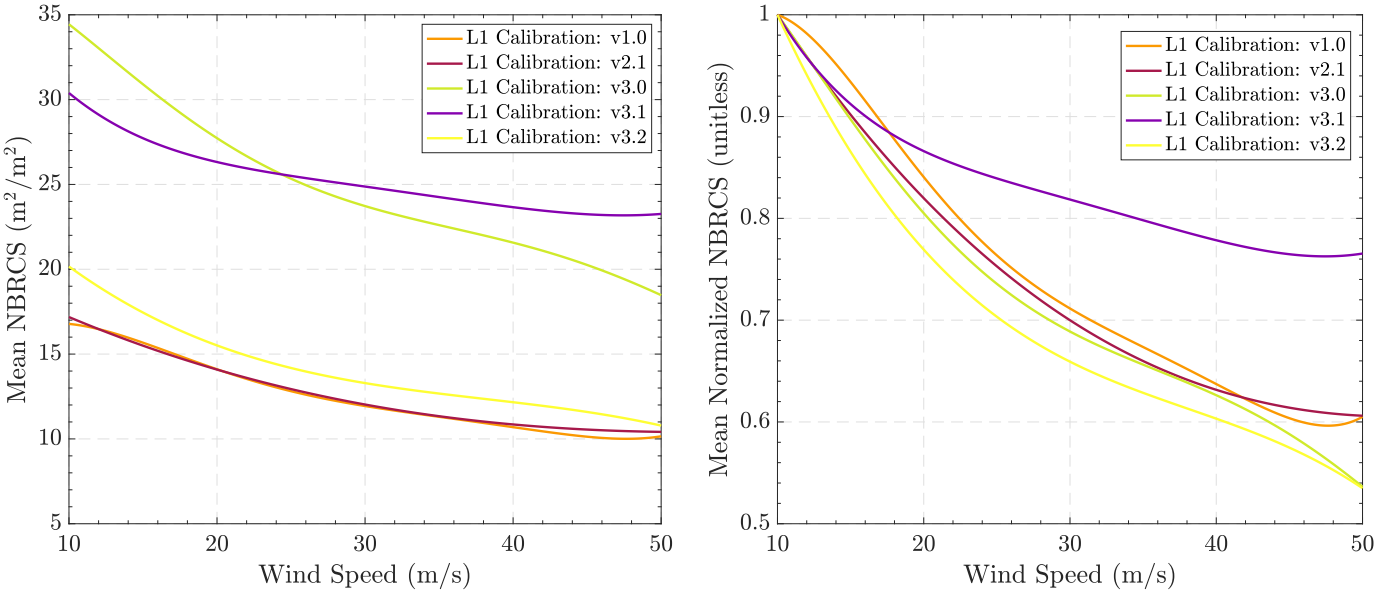

(a) (b)

Fig. 6: Mean CYGNSS NBRCS binned by reference wind speed. Reference wind speed estimates are locally generated using the Willoughby parametric storm model informed by 610 cyclones in the IBTrACS dataset. (a) Mean CYGNSS NBRCS vs wind speed (b) Mean CYGNSS NBRCS vs wind speed normalized by value at wind speed 10 m/s

deviation σ_{NBRCS} of the NBRCS in each bin computed; results for μ_{NNRCS} are shown in Figure 6(a).

The results show that μ_{NBRCS} values for both the v3.0 and v3.1 data are consistently higher across all wind speeds when compared to other data versions. Because a constant shift across all wind speeds can be accounted for in any corresponding GMF for each product, these shifts have little impact on wind speed retrieval. Figure 6(b) plots the results of plot (a) divided by the value at wind speed 10 m/s to emphasize the wind speed dependence of each product. For wind speeds in the 40-50 m/s range, the sensitivity of the v3.0 NBRCS to wind speed appears to be greatest (achieving a slope of 0.36 (m^2/m^2)/(m/s), with v3.2 having the next highest, and v3.1 the least (a slope of 0.05 (m^2/m^2)/(m/s), an 86% reduction relative to v3.0.) The differences in product performance for high wind speeds revealed by use of the IBTrACS/Willoughby approach indicates the utility of the method in product development and assessment.

The NBRCS standard deviation normalized by its mean ($\sigma_{NBRCS}/\mu_{NBRCS}$) can also be examined as a function of wind speed as shown in Figure 7. Smaller values of this parameter indicate reduced variability in the data within a specific wind speed bin and should be expected to improve the accuracy of downstream wind speed retrievals. Sources of variability in a bin include the impacts of incidence angle, inhomogeneous ocean conditions, inaccuracies in the matchup datasets, speckle and thermal noise errors, calibration uncertainties, and/or other effects.

The results in Figure 7 show for wind speeds 10-30 m/s that the v3.1 approach delivers the least uncertainty (≈0.35 on average) while the v1.0 approach has the greatest uncertainty (≈0.5 average). These results seem reasonable given the

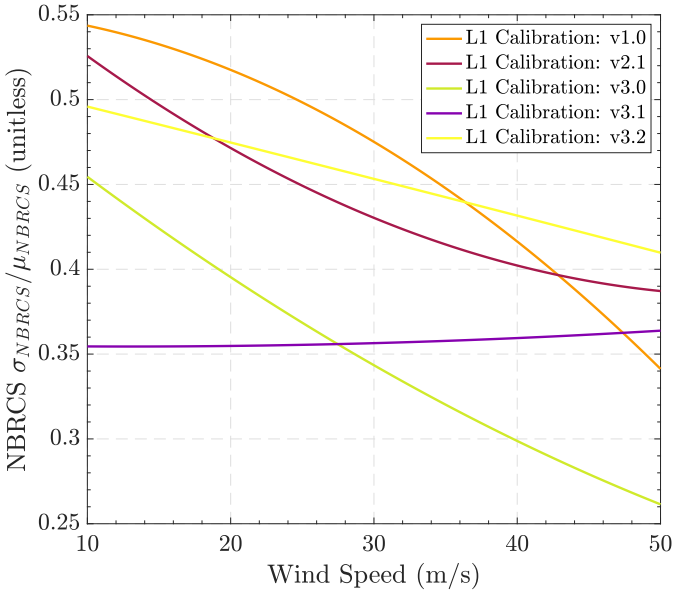

Fig. 7: Different versions of CYGNSS NBRCS ($\sigma_{NBRCS}/\mu_{NBRCS}$) binned by reference wind speed. Reference wind speed estimates are locally generated using the Willoughby parametric storm model informed by the IBTrACS dataset. Local wind predictions used to bin CYGNSS's observations span a total of 610 storms

prelaunch antenna patterns used in v1.0 that provide only an approximation of the on-board antenna patterns and therefore introduce greater variability. For wind speeds 40-50 m/s, v3.0 and v3.2 show the lowest $\sigma_{NBRCS}/\mu_{NBRCS}$ values of ≈0.275 and ≈0.380. When combined with the improved high wind sensitivity of μ_{NBRCS} for these products, the continued improvements in product performance are evident. Table II

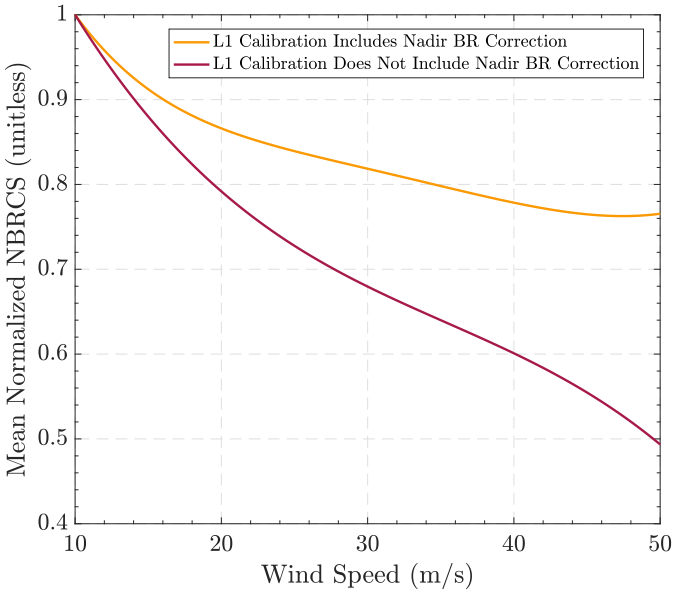

Fig. 8: Normalized mean CYGNSS NBRCS vs reference wind speeds with/without nadir bin ratio corrections (NC_{NDR}). All other elements of their respective calibration schemes are identical and mimic v3.2

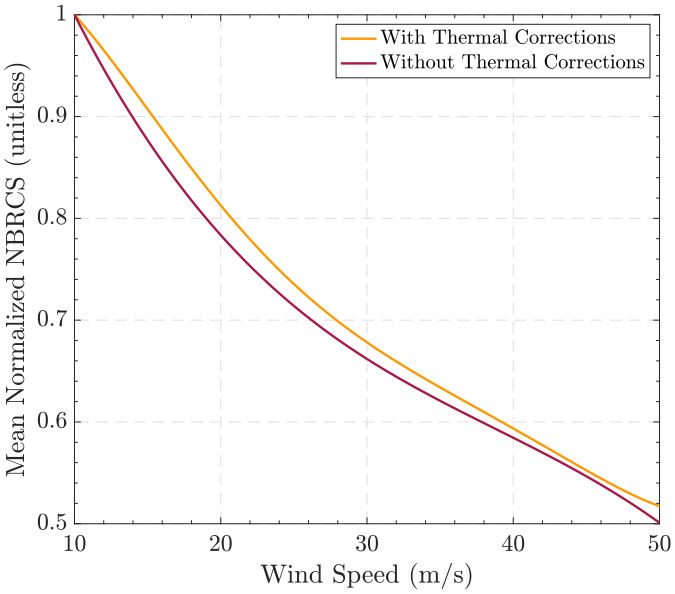

Fig. 9: Normalized mean CYGNSS NBRCS vs reference wind speeds with/without corrections intended to minimize effects of thermal dependencies. All other elements of their respective calibration schemes are identical and mimic v3.2

summarizes the high wind slope and $\sigma_{NBRCS}/\mu_{NBRCS}$ metrics for the 40-50 m/s wind speed range for all the products considered.

Note that the analyses of this Section do not focus on "true" NBRCS values but rather on the wind speed sensitivity and variability of these products that can be revealed by incorporating the IBTrACS/Willoughby matchup dataset.

B. Use For Level-1 Calibration Tuning

The IBTRaCS/Willoughby matchup dataset can also be used to assess the impact of specific calibration corrections within a given data release as part of the development of the release. As discussed in [13] and [14], interference from other spaceborne transmitters necessitates the inclusion of the bin ratio correction in estimating system noise levels. This correction was incorporated as part of the v3.1 approach prior to the use of the IBTRaCS/Willoughby matchup dataset for high wind analyses.

Figure 8 illustrates μ_{NBRCS} values versus wind speed for two v3.1-like approaches including or excluding the bin-ratio correction for the nadir antenna. While including the correction was found in other analyses to reduce the impact of external sources of interference, Figure 8 shows that the correction has the undesired impact of reducing wind speed sensitivity by up to 75% at higher wind speeds as found in other references [37]. This correction is therefore not included in CYGNSS's upcoming v3.2 data release. The reduction in high wind sensitivity caused by the previous bin ratio correction is hypothesized to involve a coupling of signal intensity and noise levels that causes signal compression effects and gain correction uncertainties. The development of an improved correction using the in-orbit LNA gain settings is currently underway.

TABLE II: Estimates of mean CYGNSS NBRCS sensitivity and normalized uncertainty over a wind speed range of 40-50 m/s across different Level-1 calibration schemes. Reference wind speed estimates are locally generated using the Willoughby parametric storm model informed by the IBTrACS dataset

Data Version	$\lvert d\sigma_0/du_{10}\rvert$	$\sigma_{NBRCS}/\mu_{NBRCS}$
v1.0	0.08	0.37
v2.1	0.05	0.39
v3.0	0.36	0.28
v3.1	0.05	0.36
v3.2	0.16	0.27

Figure 9 presents results from a second study of a v3.2-like approach applied with and without thermal corrections. These corrections are implemented using a temperature-dependent zenith LNA gain LUT found to reduce the magnitude of temperature dependencies that cause 40-60 day temporal oscillations of CYGNSS observables. In this case the modification has only a small impact on NBRCS sensitivity, with mean pre-correction slopes of ≈0.19 (m^2/m^2)/(m/s) reducing only to ≈0.17 (m^2/m^2)/(m/s) post-correction. These results have motivated the inclusion of the thermal correction as part of the upcoming v3.2 CYGNSS L1 data release.

C. Use For L2 Algorithm Development

The μ_{NBRCS} curves versus wind speed obtained using the IBTRaCS/Willoughby matchup dataset (see Fig. 6) can also be applied in a zeroth-order study of the potential wind speed retrieval performance of specific products. Figure 10 plots the NBRCS and corresponding inverted wind speeds (labeled the "synthetic storm GMF" wind speeds) for a sample CYGNSS track crossing Hurricane Walaka in 2018 using a v3.2 Level-1

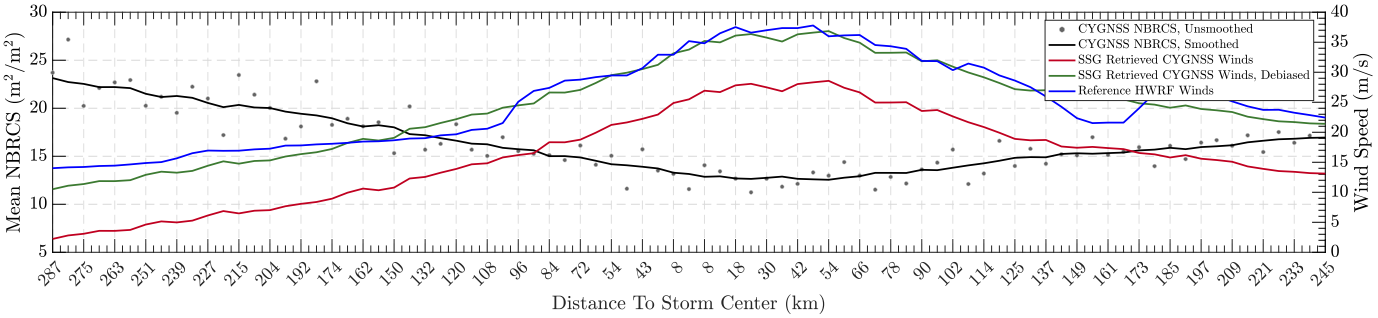

Fig. 10: Example Level-2 wind speed retrieval using synthetic storm GMF (SSG) for a CYGNSS track observing Hurricane Walaka on DOY 275, 2018 at approximately 12:00:00 UTC. A v3.2 calibration is applies to NBRCS

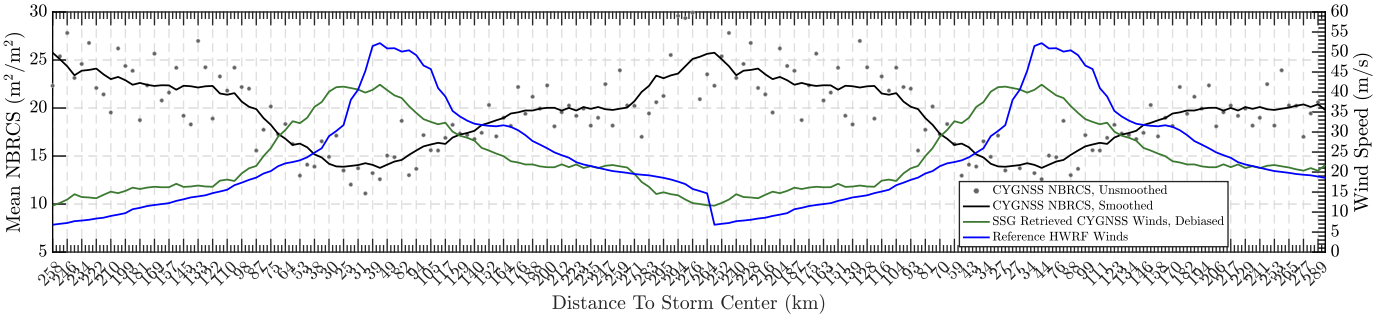

Fig. 11: Level-2 wind speed retrieval using synthetic storm GMF (SSG) for a CYGNSS track observing a Cat. 3 Hurricane on DOY 283, 2018. Along track retrieved wind speed correlation is 85% and uRMSE relative to storm maximum winds at the time of observation is 7.70%

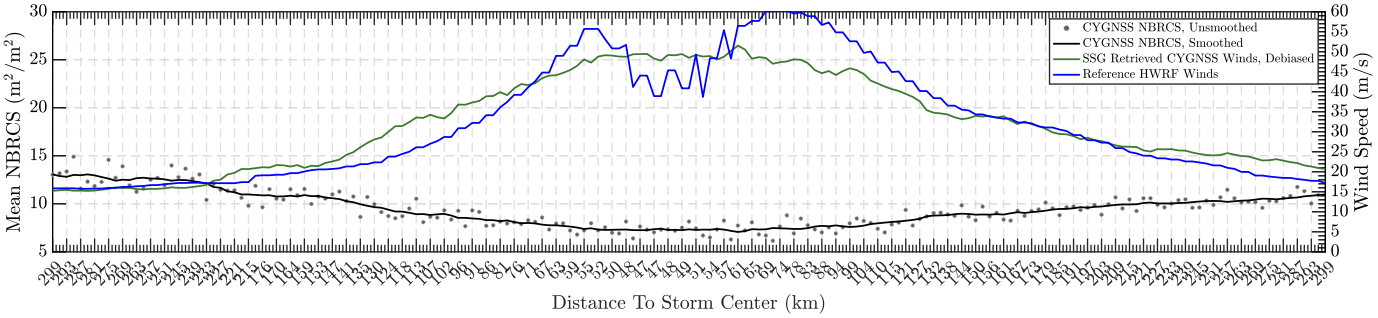

Fig. 12: Level-2 wind speed retrieval using synthetic storm GMF (SSG) for a CYGNSS track observing a Cat. 4 Hurricane on DOY 249, 2021. Along track retrieved wind speed correlation is 86% and uRMSE relative to storm maximum winds at the time of observation is 10.77%

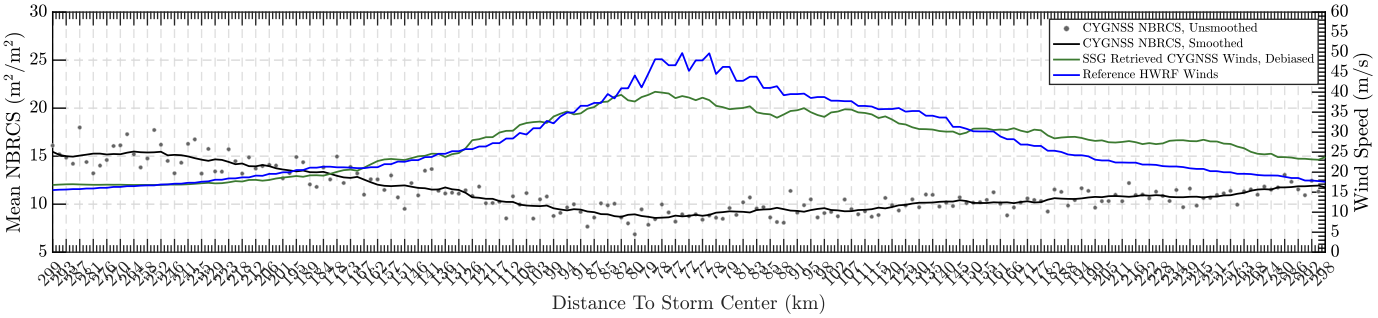

Fig. 13: Level-2 wind speed retrieval using synthetic storm GMF (SSG) for a CYGNSS track observing a Cat. 4 Hurricane on DOY 250, 2021. Along track retrieved wind speed correlation is 81% and uRMSE relative to storm maximum winds at the time of observation is 10.18%

calibration algorithm; reference HWRF wind speeds are also included for comparison. The correlation between retrieved and reference wind speeds for this track is 97% despite an 8.25 m/s reduction in the mean wind speed in the retrieved

product. The root-mean-square-error (RMSE) over the track is 9.18 m/s and the unbiased-RMSE is 1.78 m/s. These results again demonstrate the utility of the IBTRaCS/Willoughby matchup dataset and the potential for its use in continuing improvements of both the Level-1 and Level-2 products of the CYGNSS mission. It is also of interest to explore retrieval performance over storms with a higher level of development. To further highlight the utility of the proposed approach in the context of L2 algorithm development activities, Figs 11-13 depict observed trends for additional storms observed by CYGNSS for which reference HWRF wind fields were available for validation and where the level of storm development, at the time of observation, was equivalent to a Cat 3. Hurricane or greater. The debiasing factors for each track were found to be dependent on specific observation geometry and level of storm development, ranging between 0.5-9 m/s. Along track correlations of retrieved wind speeds range between 73-81% with an uRMSE relative to the storm's maximum wind at the time of observation on the order of 7.70-10.77%. To provide context, the CYGNSS mission requirement is 10% retrieval error.

VI. Conclusion

The utility of an alternate high wind reference dataset in the context of GNSS-R ocean wind speed remote sensing algorithm development, assessment, and validation was presented in this paper. The results indicate clear correlations between CYGNSS NBRCS and simulated surface winds highlighting the utility of integrating such models as part of standard algorithm development and calibration assessment practices. The IBTRaCS/Willoughby model considered represents only one example of the method, and future studies may consider incorporating more sophisticated models that may more accurately capture storm structure and thereby further improve matchup datasets.

References

[1] M. Asgarimehr, C. Arnold, T. Weigel, C. Ruf, and J. Wickert, "GNSS reflectometry global ocean wind speed using Deep Learning: Development and assessment of cygnssnet," Remote Sensing of Environment, vol. 269, p. 112801, 2022.

[2] M. C. Evans and C. S. Ruf, "Toward the detection and imaging of ocean microplastics with a spaceborne radar," IEEE Transactions on Geoscience and Remote Sensing, vol. 60, pp. 1–9, 2022.

[3] Z. Pu, Y. Wang, X. Li, C. Ruf, L. Bi, and A. Mehra, "Impacts of assimilating CYGNSS satellite ocean-surface wind on prediction of landfalling hurricanes with the HWRF model," Remote Sensing, vol. 14, no. 9, p. 2118, 2022.

[4] F. Said, Z. Jelenak, J. Park, and P. S. Chang, "The NOAA track-wise wind retrieval algorithm and product assessment for CyGNSS," IEEE Transactions on Geoscience and Remote Sensing, vol. 60, pp. 1–24, 2022.

[5] M. M. Al-Khaldi, A. Bringer, and J. T. Johnson, "Studies of a rapid change detector using CYGNSS level-2 wind speed products," IEEE Journal of Selected Topics in Applied Earth Observations and Remote Sensing, vol. 14, pp. 7931–7937, 2021.

[6] W. Guo, H. Du, J. W. Cheong, B. J. Southwell, and A. G. Dempster, "GNSS-R wind speed retrieval of sea surface based on particle swarm optimization algorithm," IEEE Transactions on Geoscience and Remote Sensing, vol. 60, pp. 1–14, 2022.

[7] C. Ruf et al., "Cyclone Global Navigation Satellite System," Michigan Publishing, University of Michigan, Ann Arbor, MI, 2022.

[8] S. Gleason, C. S. Ruf, M. P. Clarizia, and A. J. O'Brien, "Calibration and unwrapping of the normalized scattering cross section for the Cyclone Global Navigation Satellite System," IEEE Transactions on Geoscience and Remote Sensing, vol. 54, no. 5, pp. 2495–2509, 2016.

[9] R. Balasubramaniam and C. Ruf, "Characterization of rain impact on L-band GNSS-R ocean surface measurements," Remote Sensing of Environment, vol. 239, p. 111607, 2020.

[10] C. Ruf, R. Atlas, P. Chang, M. Clarizia, J. Garrison, S. Gleason, S. Katzberg, Z. Jelenak, J. Johnson, S. Majumdar, A. O'brien, D. Posselt, A. Ridley, R. Rose and V. Zavorotny, "New Ocean Winds Satellite Mission to Probe Hurricanes and Tropical Convection," *Bulletin of the American Meteorological Society*, vol. 97, no. 3, pp. 385-395, 2016.

[11] M. M. Al-Khaldi, S. J. Katzberg, J. T. Johnson, Y. Kang, E. J. Kubatko, and S. Gleason, "Matched filter cyclone maximum wind retrievals using CYGNSS: Progress update and error analysis," IEEE Journal of Selected Topics in Applied Earth Observations and Remote Sensing, vol. 14, pp. 3591–3601, 2021.

[12] S. Gleason, C. S. Ruf, A. J. O'Brien, and D. S. McKague, "The CYGNSS level 1 calibration algorithm and error analysis based on on-orbit measurements," IEEE Journal of Selected Topics in Applied Earth Observations and Remote Sensing, vol. 12, no. 1, pp. 37–49, 2019.

[13] S. Gleason, J. Johnson, C. Ruf, and C. Bussy-Virat, "Characterizing background signals and noise in spaceborne GNSS reflection ocean observations," IEEE Geoscience and Remote Sensing Letters, vol. 17, no. 4, pp. 587–591, 2020.

[14] S. Gleason, M. M. Al-Khaldi, C. S. Ruf, D. S. McKague, T. Wang, and A. Russel, "Characterizing and mitigating digital sampling effects on the CYGNSS level 1 calibration," IEEE Transactions on Geoscience and Remote Sensing, vol. 60, pp. 1–12, 2022.

[15] T. Wang, C. S. Ruf, B. Block, D. S. McKague, and S. Gleason, "Design and performance of a GPS constellation Power Monitor system for improved CYGNSS L1b calibration," IEEE Journal of Selected Topics in Applied Earth Observations and Remote Sensing, vol. 12, no. 1, pp. 26–36, 2019.

[16] T. Wang, C. S. Ruf, S. Gleason, A. J. O'Brien, D. S. McKague, B. P. Block, and A. Russel, "Dynamic calibration of GPS effective isotropic radiated power for GNSS-reflectometry earth remote sensing," IEEE Transactions on Geoscience and Remote Sensing, vol. 60, pp. 1–12, 2022.

[17] C. S. Ruf, S. Gleason, and D. S. McKague, "Assessment of CYGNSS wind speed retrieval uncertainty," IEEE Journal of Selected Topics in Applied Earth Observations and Remote Sensing, vol. 12, no. 1, pp. 87–97, 2019.

[18] S. Gleason, M. Al-Khaldi, C. Ruf, D. McKague, T. Wang and A. Russel, "Summary of Changes in the v3.1 L1 Calibration," *NASA CYGNSS Science Team Meeting*, Jul 2021, Ann Arbor, MI.

[19] V. Zavorotny and A. Voronovich, "Scattering of GPS signals from the ocean with wind remote sensing application," *IEEE Transactions on Geoscience and Remote Sensing*, vol. 38, no. 2, pp. 951-964, 2000.

[20] A. G. Voronovich and V. U. Zavorotny, "Bistatic radar equation for signals of opportunity revisited," *IEEE Transactions on Geoscience and Remote Sensing*, vol. 56, No.3, pp. 1959-1968, April, 2018.

[21] Ruf, C., R. Balasubramaniam, "Development of the CYGNSS Geophysical Model Function for Wind Speed," IEEE J. Sel. Topics Appl. Earth Obs. Remote Sens., doi: 10.1109/JSTARS.2018.2833075, 2018.

[22] S. Katzberg, J. Dunion and G. Ganoe, "The use of reflected GPS signals to retrieve ocean surface wind speeds in tropical cyclones," *Radio Science*, vol. 48, no. 4, pp. 371-387, 2013.

[23] S. Katzberg, O. Torres and G. Ganoe, "Calibration of reflected GPS for tropical storm wind speed retrievals," *Geophysical Research Letters*, vol. 33, no. 18, 2006.

[24] Hersbach, H. et al. (2020) "The ERA5 global reanalysis," Quarterly Journal of the Royal Meteorological Society, 146(730), pp. 1999–2049.

[25] I. G. Fernandes, F. M. Pimenta, O. R. Saavedra, and A. R. Silva, "Offshore validation of ERA5 reanalysis with hub height wind observations of Brazil," 2021 IEEE PES Innovative Smart Grid Technologies Conference - Latin America (ISGT Latin America), 2021.

[26] Sirui Lv, Wenming Lin, Zhixiong Wang, et al., "Blending Sea Surface Winds from the HY-2 Satellite Scatterometers Based on a 2D-Var Method," *Remote Sensing*, 15(1), 193, 2023

[27] X. Li, J. Yang, G. Han, L. Ren, G. Zheng, P. Chen, and H. Zhang, "Tropical Cyclone Wind Field Reconstruction and validation using measurements from SFMR and SMAP radiometer," *Remote Sensing*, vol. 14, no. 16, p. 3929, 2022.

[28] E. Uhlhorn, P. Black, J. Franklin, M. Goodberlet, J. Carswell and A. Goldstein, "Hurricane Surface Wind Measurements from an Operational

Stepped Frequency Microwave Radiometer," *Monthly Weather Review*, vol. 135, no. 9, pp. 3070-3085, 2007.
[29] A. T. Cox and V. J. Cardone, "20 Years of Operational Forecasting at Oceanweather," *7th International Workshop on Wave Hindcasting and Forecasting*, 2002, Alberta, Canada.
[30] D. C. Yan and T. Y. Zhang, "Research progress on tropical cyclone parametric wind field models and their application," Regional Studies in Marine Science, vol. 51, p. 102207, 2022.
[31] L. Vijayan, W. Huang, K. Yin, E. Ozguven, S. Burns, and M. Ghorbanzadeh, "Evaluation of parametric wind models for more accurate modeling of storm surge: A case study of hurricane michael," Natural Hazards, vol. 106, no. 3, pp. 2003–2024, 2021.
[32] W.-T. Chao and C.-C. Young, "Accurate storm surge prediction with a parametric cyclone and neural network hybrid model," Water, vol. 14, no. 1, p. 96, 2022.
[33] H. Willoughby and M. Rahn, "Parametric Representation of the Primary Hurricane Vortex. Part I: Observations and Evaluation of the Holland (1980) Model," *Monthly Weather Review*, vol. 132, no. 12, pp. 3033-3048, 2004.
[34] H. Willoughby, R. Darling and M. Rahn, "Parametric Representation of the Primary Hurricane Vortex. Part II: A New Family of Sectionally Continuous Profiles," *Monthly Weather Review*, vol. 134, no. 4, pp. 1102-1120, 2006.
[35] F. Said, S. Katzberg and S. Soisuvarn, "Retrieving Hurricane Maximum Winds Using Simulated CYGNSS Power-Versus-Delay Waveforms," *IEEE Journal of Selected Topics in Applied Earth Observations and Remote Sensing*, vol. 10, no. 8, pp. 3799-3809, 2017.
[36] K. R. Knapp, M. C. Kruk, D. H. Levinson, H. J. Diamond, and C. J. Neumann, "The International Best Track Archive for Climate Stewardship (ibtracs)," Bulletin of the American Meteorological Society, vol. 91, no. 3, pp. 363–376, 2010.
[37] S. Gleason, M. Al-Khaldi, C. Ruf, D. McKague, R. Balasubramaniam, T. Wang and A. Russel, "L1 Cal Update," *NASA CYGNSS Science Team Meeting*, Aug 2022, Ann Arbor, MI.

Mohammad M. Al-Khaldi received the bachelor's degree in electrical engineering from the American University of Sharjah, Sharjah, United Arab Emirates, in 2015, the M.S. degree in electrical engineering from Texas A&M University, College Station, TX, USA, in 2017, and the M.S. degree in electrical and computer engineering from The Ohio State University, Columbus, OH, USA, in 2019, where he completed his Ph.D. degree with the Department of Electrical and Computer Engineering and ElectroScience Laboratory in 2020. Dr. Al-Khaldi was previously a Project Scientist I, Post-doctoral Fellow II and Post-doctoral Fellow I at the University Corporation for Atmospheric Research's (UCAR's) COSMIC Program in Boulder, CO, USA. He is currently a Senior Research Associate at The Ohio State University's ElectroScience Laboratory and Department of Electrical and Computer Engineering.

Dr. Al-Khaldi is a member of the NASA CYGNSS mission science team, NASA CYGNSS mission calibration and validation team, IEEE GRSS Technical Committee on Modeling in Remote Sensing, IEEE GRSS Technical Committees on Frequency Allocations in Remote Sensing, is an associate member of commissions B and F of the International Union of Radio Science (URSI), is a NASA CSDA GNSS-R Subject Matter Expert (SME) and serves as an Associate Editor of Radio Science.

His current research interests include applied electromagnetics, rough surface scattering, and spaceborne remote sensing.

Scott Gleason received the B.S. degree in electrical and computer engineering from the State University of New York at Buffalo, Buffalo, NY,USA, the M.S. degree in engineering from Stanford University, Stanford, CA, USA, and the Ph.D. degree in applied physics from the University of Surrey, Surrey, U.K., in 1991, 1999 and 2007, respectively. He is currently the President of the Daaxa LLC consulting company, specializing in GNSS instruments, calibration and remote sensing applications. He is a Co-Investigator on the science team and Instrument Scientist for the NASA CYGNSS mission. He has worked in the areas of astronautics, remote sensing and global navigation satellite systems for more than 20 years, including at NASAs Goddard Space Flight Center, Stanford's GPS Laboratory, Surrey Satellite Technology Limited, Concordia University (Montreal, Canada), Southwest Research Institute, the University Corporation for Atmospheric Research and the National Oceanography Centre, Southampton, U.K.

Joel T. Johnson received the bachelor's degree in electrical engineering degree from the Georgia Institute of Technology, Atlanta, GA, USA, in 1991, and the S.M. and Ph.D. degrees from the Massachusetts Institute of Technology, Cambridge, MA, USA, in 1993 and 1996, respectively.

He is currently a Professor with the ElectroScience Laboratory, Department of Electrical and Computer Engineering, The Ohio State University, Columbus, OH, USA. His current research interests include the areas of microwave remote sensing, propagation, and electromagnetic wave theory.

Dr. Johnson is a member of commissions B and F of the International Union of Radio Science (URSI), Tau Beta Pi, Eta Kappa Nu, and Phi Kappa Phi. He received the 1993 Best Paper Award from the IEEE Geoscience and Remote Sensing Society, was named an Office of Naval Research Young Investigator, the National Science Foundation Career Awardee, the PECASE Award Recipient in 1997, and was recognized by the U.S. National Committee of URSI as a Booker Fellow in 2002. He served as Technical Program Co-Chair for the 2017 International Geoscience and Remote Sensing Symposium. He has served as an Associate Editor for the Transactions on Geoscience and Remote Sensing since 2000. He is also a Past Chair of the GRSS Technical Committee on Frequency Allocations in Remote Sensing.

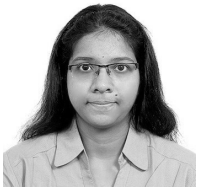

Rajeswari Balasubramaniam received the B.E. degree in electrical and electronics engineering from Anna University, Chennai, India, in 2014, the M.E. degree in geoinformatics with a specialization in remote sensing and image processing from the Indian Institute of Space Science and Technology, Thiruvananthapuram, India, in 2016, Ph.D. degree from the Department of Climate and Space Sciences and Engineering, University of Michigan, Ann Arbor, MI, USA.

Her current work focuses on various aspects of calibration and validation for the NASA Cyclone Global Navigation Satellite System mission. Her research interests include GNSS-reflectometry, statistical signal processing, remote sensing inversion theory, data analysis, and microwave engineering

Christopher S. Ruf received the B.A. degree in physics from Reed College, Portland, OR, and the Ph.D. degree in electrical and computer engineering from the University of Massachusetts at Amherst. He is currently Professor of atmospheric science and space engineering at the University of Michigan; and Principal Investigator of the Cyclone Global Navigation Satellite System NASA Earth Venture mission. He has worked previously at Intel Corporation, Hughes Space and Communication, the NASA Jet Propulsion Laboratory, and Penn State University. His research interests include GNSS-R remote sensing, microwave radiometry, atmosphere and ocean geophysical retrieval algorithm development, and sensor technology development. Dr. Ruf is a member of the American Geophysical Union (AGU), the American Meteorological Society (AMS), and Commission F of the Union Radio Scientifique Internationale. He is former Editor-in-Chief of the IEEE Transactions on Geoscience and Remote Sensing and has served on the editorial boards of Radio Science and the Journal of Atmospheric and Oceanic Technology. He has been the recipient of four NASA Certificates of Recognition and seven NASA Group Achievement Awards, as well as the 1997 TGRS Best Paper Award, the 1999 IEEE Resnik Technical Field Award, the 2006 IGARSS Best Paper Award, and the 2014 IEEE GRSS-S Outstanding Service Award.

Darren S. McKague received the Ph.D. degree in Astrophysical, Planetary, and Atmospheric Sciences from the University of Colorado, Boulder, in 2001. He is an Associate Research Scientist in the Department of Climate and Space Sciences and Engineering at the University of Michigan. Prior to working for Michigan, he worked as a systems engineer for Ball Aerospace and for Raytheon, and as a research scientist at Colorado State University. His work has focused on remote sensing with emphases on the development of space-borne microwave remote sensing hardware, microwave remote sensor calibration techniques, and on mathematical inversion techniques for geophysical retrievals. His experience with remote sensing hardware includes systems engineering for several advanced passive and active instrument concepts and the design of the calibration subsystem on the Global Precipitation Mission (GPM) Microwave Imager (GMI) as well as the development of calibration and inter-calibration techniques for the GPM constellation. His algorithm experience includes the development of a near-real time algorithm for the joint retrieval of water vapor profiles, temperature profiles, cloud liquid water path, and surface emissivity for the Advanced Microwave Sounding Unit (AMSU) at Colorado State University, and the development of the precipitation rate, precipitation type, sea ice, and sea surface wind direction algorithms for the risk reduction phase of the Conical scanning Microwave Imager/Sounder (CMIS).

Bachir Annane received the Diplôme d'enseignement Supérieur en Mathématique pure (DES in pure mathematics) from the University of Algiers (USTHB), Bab Ezzouar, Algeria in 1988. He later went on to earn an M.S. degree in applied mathematics from the University of Central Florida, Orlando, FL, USA in 1993, and M.S. and Ph.D. degrees in meteorology from Florida State University, Tallahassee, FL, USA in 1997 and 2019, respectively. Since 2005, Bachir Annane has been a Researcher with the Univ. of Miami/CIMAS and NOAA/AOML/HRD, Miami, FL 33149 USA.

Tianlin Wang received the B.E. degree in electrical engineering from the East China University of Science and Technology, the M.S. degree in radio physics from Fudan University, and the M.S. and Ph.D. degrees in electrical engineering from the University of Michigan, Ann Arbor. He is currently a President's Postdoctoral Scholar in the Department of Electrical and Computer Engineering and ElectroScience Laboratory of The Ohio State University. His research interests include wave propagation and scattering, microwave remote sensing, microwave measurements, and radio frequency (RF) circuits.

Dr. Wang is a member of Tau Beta Pi, Eta Kappa Nu, American Geophysical Union (AGU), and Institute of Navigation (ION) and an Early Career Member of Commission F of the U.S. National Committee (USNC) for the Union Radio Scientifique Internationale (URSI). He received the 2018 IEEE Mikio Takagi Student Prize, an Outstanding Student Presentation Award at the 2018 AGU Fall Meeting, the 2020 Richard F. and Eleanor A. Towner Prize for Distinguished Academic Achievement and Distinguished Leadership Award from the University of Michigan, and the 2021 Ernest K. Smith USNC-URSI Student Prize (2nd Place). He is a recipient of the 2020 President's Postdoctoral Scholars Program (PPSP) Fellowship from The Ohio State University and the 2021 Mistletoe Research Fellowship from the Momental Foundation. He is currently serving as a co-chair of the IEEE Geoscience and Remote Sensing Society (GRSS) Technical Committee on Modeling in Remote Sensing, a member of the GRSS Chapters committee, and a member of the GRSS Young Professionals committee.

Anthony Russel received the B.S. degree in computer science engineering from Michigan State University, East Lansing, MI, USA, in 2014. He is a member of the engineering staff with the Space Physics Research Laboratory, College of Engineering, University of Michigan, Ann Arbor, MI, USA. His primary engineering activities involve algorithm development and large-scale data processing as a member of the Science Operations Center for the CYGNSS mission.

Dorina Twigg received a B.S.E. degree in computer engineering from the University of Michigan, Ann Arbor, MI, USA, an M.S. degree in computer science from Wayne State, Detroit, MI USA, in 2012. She is a member of the engineering staff with the Space Physics Research Laboratory, College of Engineering, University of Michigan, Ann Arbor, MI, USA, and has a lead role in satellite commanding and scientific data processing with the Science Operations Center for the CYGNSS NASA Earth Venture mission.